Experimental Demonstration of Fractional-Order Oscillators of Orders 2.6 and 2.7

A. S. Elwakil[a,b,*], A. Agambayev[c], A. Allagui[e,f], K. N. Salama[c,d]

[a] Dept. of Electrical and Computer Engineering, University of Sharjah, PO Box 27272, Sharjah, United Arab Emirates
[b] Nanoelectronics Integrated Systems Center (NISC), Nile University, Cairo, Egypt
[c] Computer, Electrical and Mathematical Sciences and Engineering Division, King Abdullah University of Science and Technology (KAUST), Thuwal, Saudi Arabia
[d] The Neuroscience Research Institute, The Ohio State University, Columbus, OHIO, USA
[e] Dept. of Sustainable and Renewable Energy Engineering, University of Sharjah, PO Box 27272, Sharjah, United Arab Emirates
[f] Advanced Materials Research Center, University of Sharjah, PO Box 27272, Sharjah, United Arab Emirates

Abstract

The purpose of this work is to provide an experimental demonstration for the development of sinusoidal oscillations in a fractional-order Hartley-like oscillator. The solid-state fractional-order electric double-layer capacitors were first fabricated using graphene-percolated P(VDF-TrFE-CFE) composite structure, and then characterized by using electrochemical impedance spectroscopy. The devices exhibit the fractional orders of 0.6 and 0.74 respectively (using the model $Z_c = R_s + 1/(j\omega)^\alpha C_\alpha$), with the corresponding pseudocapacitances of approximately $93\,nF\sec^{-0.4}$ and $1.5\,nF\sec^{-0.26}$ over the frequency range $200\,kHz - 6\,MHz$ ($R_s < 15\,\Omega$). Then, we verified using these fractional-order devices integrated in a Hartley-like circuit that the fractional-order oscillatory behaviors are of orders 2.6 and 2.74.

Keywords: Fractional-order oscillator, Fractional-order capacitor, Hartley oscillator, Constant Phase Element,

1. Introduction

In recent years, considerable interest has been devoted to the use of fractional-order calculus in several areas of science and engineering, including viscoelasticity [1], boundary layer defects in ducts [2], fractional kinetics [3], electrode-electrolyte interfacial processes [4], and many other systems [5–7]. Fractional-order electrical oscillators, in particular, were introduced in [8] where a classical Wien-bridge oscillator was studied in the event that its two ideal capacitors are replaced by fractional-order capacitors. In these capacitors, the time-domain current-voltage relationship is given by the fractional-order derivative:

$$i = C_\alpha \frac{d^\alpha v}{dt^\alpha}$$

where α is the order of differentiation, also known as the dispersion coefficient ($0 < \alpha < 1$), and C_α is the pseudocapacitance measured in units of $\mathrm{F}\sec^{\alpha-1}$.

When one (or more) of these capacitors is employed with other components in a circuit, it is described by a set of fractional-order differential equations in the time domain [21, 22]. However, applyinb the Laplace transform is also valid for in fractional calculus which leads in the frequency-domain to an impedance $Z_c = 1/(j\omega)^\alpha C_\alpha$ [9] where

$$(j\omega)^\alpha = \omega^\alpha \cos(\alpha\pi/2) + j\sin(\alpha\pi/2)) = R(\omega,\alpha) + jX(\omega,\alpha) \quad (1)$$

In [8] no experimental results were shown since practical fractional-order capacitors did not exist at that time. However, following the work of Biswas et al. [10], experimental tests were carried out by Radwan et al. [11] to show the existence of sinusoidal oscillations in oscillators of order $n < 2$, and verify that these oscillators operate at much higher frequencies than their integer-order counterparts due to dissipative effects. Fractional-order oscillators of order $2 < n < 3$ were conceptually studied by Radwan et al. [12], but not verified experimentally. Many other authors have demonstrated oscillatory behavior and chaos using approximate realizations of fractional-order capacitors in the form of integer-order RC-trees [13]

On the other hand, a fractional-order relaxation oscillator was first studied in [14] and experimentally verified using an RC-tree emulator of the fractional capacitor. Recently, another fractional-order relaxation oscillator [15] was studied making use of the fractional properties of some commercially available supercapacitors [16]. However, supercapacitors are mainly designed for energy storage applications and thus have large values of pseudocapacitances. Therefore, they can only be used to realize very low frequency oscillators [15]. Significant effort has been ongoing in order to fabricate well characterized fractional-order capacitors that can perform well in low and high frequencies alike while having suitably low pseudocapacitance values for various electronic circuit applications including filters

*Corresponding author
Email address: elwakil@ieee.org (A. S. Elwakil)

and oscillators [17–19].

In the present work we (i) fabricate two reduced-graphene oxide-based fractional-order capacitor devices and precisely characterize them by using an electrochemical workstation to estimate their individual fractional-orders, pseudocapacitances and the bandwidth of operation and then (ii) experimentally validate the existence of sinusoidal oscillations in a Hartley-like oscillator, which employs, in addition to the two fabricated devices two more commercial inductors (see figure 1). This means that the overall order of the oscillator is $2+\alpha$.

In this regards, the fractional-capacitors (fabricated by pressing a composite mixture of P(VDF-TrFE-CFE) polymer with appropriate amounts of reduced graphene oxide (rGO) filler between two current collectors) were found to have orders of approximately 0.6 over the frequency range $10\,kHz - 7\,MHz$ for the first device and 0.74 over the frequency range $210\,kHz - 6.5\,MHz$ for the second device. In addition, the pseudocapacitances of the devices were found to be approximately $93\,nF\,\sec^{-0.4}$ and $1.5\,nF\,\sec^{-0.26}$, respectively, with less than $15\,\Omega$ internal resistances. Hence the order of the tested oscillators are approximately 2.6 and 2.74.

2. Oscillator

2.1. Integer-order oscillator

Consider the oscillator with LC feedback shown in figure 1, which is a derivative of the Hartley oscillator. The capacitance C is considered to be ideal in this case. Assuming the two inductors are similar with inductance L and an internal parasitic resistance r, it can be shown that the characteristic equation of this oscillator is:

$$s^3 + as^2 + bs + c = 0 \tag{2}$$

where

$$\begin{aligned} a &= \tfrac{2r+R}{L} \\ b &= \tfrac{2}{LC} + \left(\tfrac{r}{L}\right)^2 + \tfrac{rR}{L^2} \\ c &= \tfrac{2r+R+R_f}{L^2C} \end{aligned} \tag{3}$$

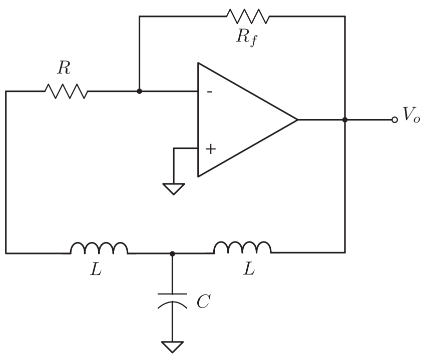

Figure 1: Hartley-based sinusoidal oscillator.

from which applying the oscillation start-up (marginal stability, i.e. $ab = c$) condition yields

$$R_f = 2r + R + \frac{rC}{L}(r+R)(2r+R) \tag{4}$$

For $R >> r$, this condition simplifies to the relation:

$$k = \frac{R_f}{R} = 1 + \frac{rC}{L}R \tag{5}$$

For ideal inductors ($r \to 0$), the start-up condition reduces to $R_f = R$ which means that the op amp is operating as a unity gain amplifier ($k = 1$). The oscillation frequency of the oscillator is given by

$$\omega_o = \sqrt{\frac{2}{LC} + \frac{r^2 + rR}{L^2}} \tag{6}$$

which simplifies to $\sqrt{2/LC}$ when $r \to 0$.

2.2. Fractional-order oscillator

Now consider replacing the ideal capacitor C in the oscillator in figure 1 with a fractional-order capacitor with impedance $Z_c = 1/(j\omega)^\alpha C_\alpha$. The characteristic equation in this case becomes

$$s^{(2+\alpha)} + as^{(1+\alpha)} + bs + cs^\alpha + d = 0 \tag{7}$$

where

$$\begin{aligned} a &= \tfrac{2r+R}{L} \\ b &= \tfrac{2}{LC_\alpha} \\ c &= \tfrac{r^2+rR}{L^2} \\ d &= \tfrac{2r+R+R_f}{L^2C_\alpha} \end{aligned} \tag{8}$$

the oscillation start-up condition and oscillation frequency can be obtained by solving the system of equations:

$$\omega^{(2+\alpha)} - \frac{a}{\tan(\frac{\alpha\pi}{2})}\omega^{(1+\alpha)} - c\omega^\alpha - \frac{b}{\sin(\frac{\alpha\pi}{2})}\omega = 0 \tag{9}$$

and

$$\frac{a}{\sin(\frac{\alpha\pi}{2})}\omega^{(1+\alpha)} + \frac{b}{\tan(\frac{\alpha\pi}{2})}\omega - d = 0 \tag{10}$$

For ideal inductors (i.e. $r \to 0$) the parameter c vanishes, and (9) simplifies to

$$\omega^{(1+\alpha)} - \frac{a}{\tan(\frac{\alpha\pi}{2})}\omega^\alpha - \frac{b}{\sin(\frac{\alpha\pi}{2})} = 0 \tag{11}$$

which, after substituting in (10), yields

$$\frac{a^2\cos(\frac{\alpha\pi}{2})}{\sin^2(\frac{\alpha\pi}{2})}\omega^\alpha + \frac{b}{\tan(\frac{\alpha\pi}{2})}\omega + \frac{ab}{\sin^2(\frac{\alpha\pi}{2})} - d = 0 \tag{12}$$

In this case, and for $\alpha = 1$, it can be readily verified that the oscillation frequency is $\sqrt{2/LC}$ with unity gain as start-up condition, as expected from the integer-order case.

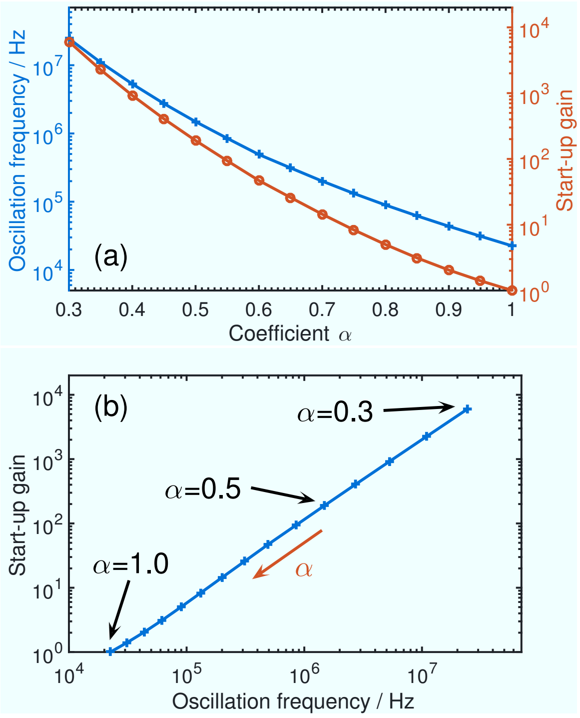

Figure 2: (a) Variation of oscillation frequency and start-up gain versus α and (b) variation of start-up gain versus oscillation frequency in the Hartley-based sinusoidal oscillator for $R = 1\,k\Omega$, $L = 10\,mH$ and $C_\alpha = 10\,nF\,\sec^{(\alpha-1)}$.

Assuming typical component values, such as $R = 1\,k\Omega$, $L = 10\,mH$, and $C_\alpha = 10\,nF\,\sec^{(\alpha-1)}$, equations (11) and (12) lead for example to the ideal oscillation frequency of $(1.488, 0.491, 0.200)$ MHz for $\alpha = (0.5, 0.6, 0.7)$ respectively, with a corresponding start-up condition given by $k = (190, 46.9, 14.4)$. Figure 2(a) is a plot of the variation of oscillation frequency and gain k versus α using these design values. The change in the oscillation frequency even for r as large as $100\,\Omega$ is found to be insignificant (less than 0.5%), and therefore (11) and (12) are sufficient for design purposes. Note however, that the start-up gain k is significantly high for $\alpha \leqslant 0.5$ (see figure 2(b)) given the gain bandwidth product (GBW) of typical op amps. For example, at $\alpha = 0.5$, an op amp with $GBW > 280\,MHz$ is required. For comparison, if an integer-order capacitor ($\alpha = 1$) of the same value of pure capacitance ($C = 10\,nF$) was employed in the design, then the resulting oscillation frequency would have been $22.50\,kHz$ with near unity start-up gain. The fact that fractional-order oscillators generate higher frequencies than their integer-order counterparts is well-known and is considered to be the main advantage of these oscillators [12]. However, this comes at a cost as shown in figure 2(b), which is the higher requirement in the start-up gain to compensate the resistive behavior embedded in the fractional-order capacitors. This does not only apply to the Hartley oscillator under study here but to all other fractional-order oscillators as well [8]. Furthermore, this high gain would imply material design considerations to be used to fabricate the fractional-order oscillators for high frequency applications.

It is worth noting that if we consider the internal resistance of the fractional-order capacitor (R_s), such that the whole component is modeled by the equivalent impedance $Z_c = R_s + 1/(j\omega)^\alpha C_\alpha$, the oscillator's characteristic equation remains the same with

$$\begin{aligned} a &= \frac{2R_s+R}{L} \\ b &= \frac{2}{LC_\alpha} \\ c &= \frac{R_s R_f}{L^2} \\ d &= \frac{R+R_f}{L^2 C_\alpha} \end{aligned} \tag{13}$$

assuming here that the inductor's internal resistor $r = 0$. Comparing (13) to (8) we note that the effect of R_s on the oscillator performance is similar to the effect r. Since we found r as large as $100\,\Omega$ to have insignificant effect on the oscillation frequency and start-up condition, we conclude that R_s will also have a similar insignificant effect if it remains less than $100\,\Omega$.

Finally, we evaluate the sensitivity of the oscillation frequency to be

$$\frac{d\omega}{\omega} = \frac{-b\cos(\frac{\alpha\pi}{2})}{a(1+\alpha)\omega^{(1+\alpha)}} \tag{14}$$

which is significantly small. For example, with the design parameters described above and at $\alpha = 0.5$, we find $d\omega/\omega = 5.18 \times 10^{-5}$.

3. Experimental

In order to conduct the experimental validation of our analysis above, fractional capacitors were fabricated by sandwiching between two platinum-coated silicon substrates a polymer-based separator formed of P(VDF-TrFE-CFE) mixed with appropriate amounts of reduced-graphene oxide (rGO) filler. rGO was obtained following a six-hour hydrothermal reduction at 180°C of GO, which was prepared using a modified Hummer's method [17, 20]. The impedance phase shift of the fractional capacitors can be tuned by adjusting the mass loading of the filler rGO material (see ref. [17] for more detail).

The electric characterization of the devices was investigated first, by using a Bio-logic VSP-300 electrochemical workstation operating in potentiostatic mode, and with $25\,mV$ ac amplitude. Subsequently, the oscillator circuit described in figure 1 was constructed using a commercial AD797 operational amplifier biased with $\pm 2\,V$ supplies. The two inductors were measured to have an inductance of $L = 1\,mH$ and internal resistance $r = 19\,\Omega$. A resistor $R >> r$ was selected to have a resistance of $1\,k\Omega$, and a variable $20\,k\Omega$-potentiometer was used for R_f in order to tune the oscillator circuit for start-up.

4. Results and discussion

Figure 3(a) shows the measured current-voltage phase shift angle which shows a nearly constant value of -54 (i.e.

$\alpha = 0.6$) extending from $10\,kHz$ up to $7\,MHz$ at different dc voltages biases with the maximum being $\pm\,200\,mV$. This constant phase behavior can be further seen from the plot of magnitude of impedance versus frequency in a log-log scale in figure 3(b), and from which we can identify a safe frequency range for operation extending from $10\,kHz$ to $6\,MHz$. The characteristic metrics of the fractional capacitors were identified using a nonlinear least-squares fitting algorithm of the impedance data with respect to the model $Z_c = R_s + 1/(j\omega)^{\alpha} C_{\alpha}$ [9]. The pseudocapacitance and dispersion coefficient values are plotted together versus the applied dc voltage in figure 3(c). The average value of C_{α} is found to be approximately $93\,nF\,\sec^{(\alpha-1)}$ with a voltage-dependent variation of approximately 8.5%. The internal resistance R_s was found always less than $15\,\Omega$ as the voltage is scanned from the limiting values -200 to $+200\,mV$.

With the selected inductors and resistors, and with $\alpha \approx 0.6$ and an average value of $C_{\alpha} = 93\,nF\,\sec^{-0.4}$, (11) predicts an oscillation frequency of approximately $449.7\,kHz$, which after substituting in (12) predicts a start-up gain of $k = 6.91$; i.e. $R_f \approx 6.91\,k\Omega$. Practically, the oscillations started at $R_f \approx 2.9\,k\Omega$. Re-calculating the oscillation frequency from (11) with this actual start-up value of R_f yields the oscillation frequency of $350.1\,kHz$ which is close enough to the measured value of $359.7\,kHz$, as shown in figure 4(a). The voltage swing across the fractional-order capacitor is about $172\,mV_{pp}$, which is within the voltage range set for the impedance spectroscopy measurements. We note that as we increase R_f, both the oscillation amplitude and the frequency increase. At $R_f \approx 5.5k\,\Omega$, the oscillation amplitude reaches approximately $600\,mV_{pp}$ and the measured frequency is $409.8\,kHz$ as shown in figure 4(b). This behaviour can also be verified using (11) and (12).

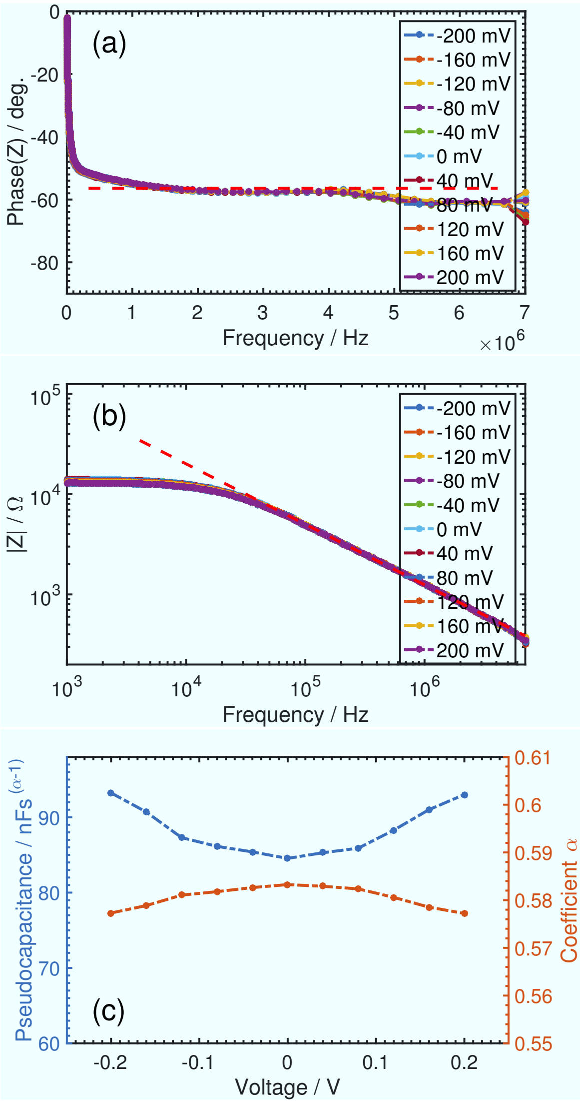

Figure 3: Impedance spectroscopy characterization of one of the fabricated fractional-order capacitor at different voltage biases: (a) variation of impedance phase angle shift versus frequency, (b) impedance magnitude response versus frequency in log-log domain, and (c) dependence of pseudocapacitance and dispersion coefficient with respect to the dc voltage biases.

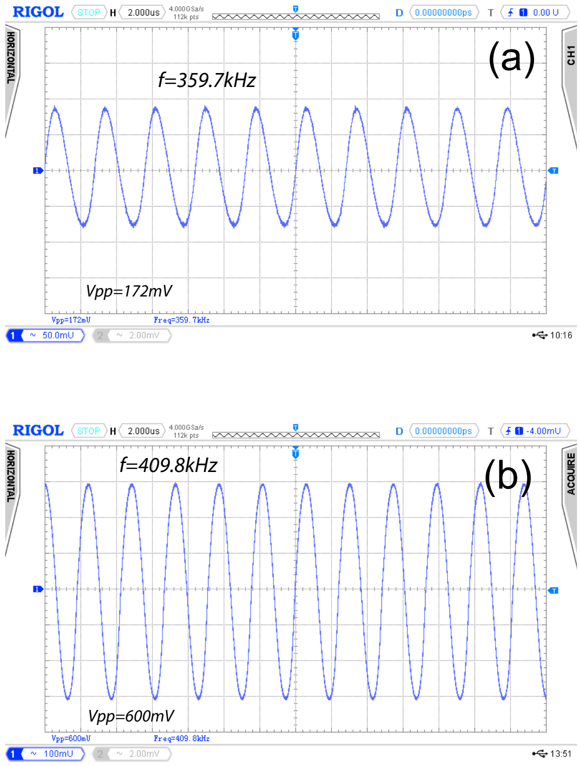

Figure 4: Experimental results for the Hartley-based sinusoidal oscillator using $1\,mH$ inductors and the fabricated fractional-order capacitor with $C_{\alpha} \approx 93\,nF\,\sec^{-0.4}$ and $\alpha \approx 0.6$ (the shown voltage is that measured directly across the fractional-order capacitor (x-axis: $2\,\mu\sec/div$, y-axis: $50\,mV/div$)).

A second fractional-order capacitor device was fabricated with another amount of rGO filler, and characterized in a similar manner. For this device, we found $\alpha \approx 0.74$ and $C_{\alpha} \approx 1.54\,nF\,\sec^{-0.26}$ over the frequency range $210kHz - 6.5MHz$. The variation of the measured phase angle versus frequency for different dc voltages is shown in figure 5(a) while a Nyquist plot is shown in figure 5(b). With these values and with $R = 1k\Omega$ and $L = 1mH$, the calculated oscillation frequency should be around $397.9kHz$ while from figure 4(c) it is measured in close agreement to be $400kHz$ with a voltage swing of approximately $300mV_{pp}$ measured across the device.

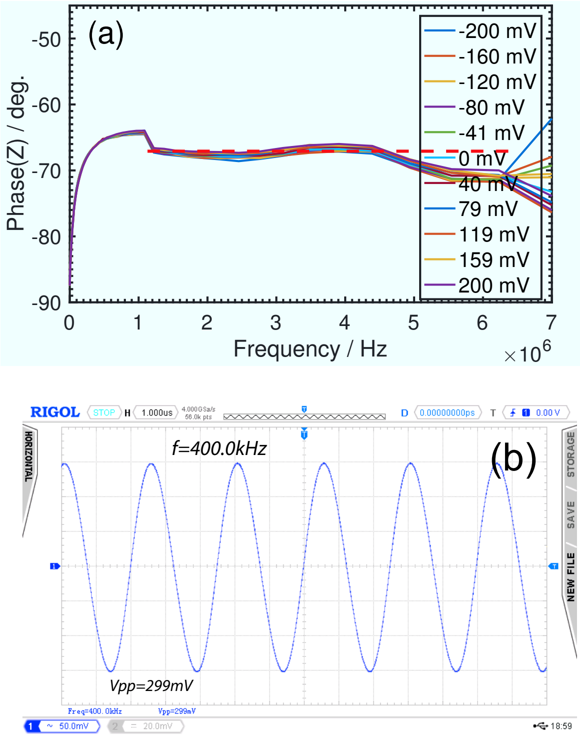

Figure 5: (a) Impedance phase shift angle of the second fabricated device versus frequency at different dc voltage biases ($C_\alpha \approx 1.54\,nF\,\text{sec}^{-0.26}$ and $\alpha \approx 0.74$) and (b) experimental results for the Hartley-based sinusoidal oscillator using $1\,mH$ inductors and the fabricated fractional-order capacitor (x-axis: $1\,\mu\text{sec}\,/div$, y-axis: $50\,mV/div$)

5. Conclusion

We have experimentally demonstrated sinusoidal oscillations generated using Hartley-like fractional-order electronic oscillators of orders 2.6 and 2.7. The order $2 < n < 3$ has been achieved thanks to the use of reduced graphene oxide-percolated P(VDF-TrFE-CFE) structures as the source of fractional capacitive behavior with constant phase shift over the frequency range $200\,kHz$–$6\,MHz$. To the best of the authors' knowledge, this is the first time in the literature that oscillations in a fractional-order electronic circuit of these orders are shown.

Acknowledgments

Two of us (ASE and AA) wish to thank the University of Sharjah for financial support (Project # 1602040634-P).

References

[1] R. Koeller, Applications of fractional calculus to the theory of viscoelasticity, Journal of Applied Mechanics 51 (2) (1984) 299–307.

[2] N. Sugimoto, Burgers equation with a fractional derivative; hereditary effects on nonlinear acoustic waves, Journal of fluid mechanics 225 (1991) 631–653.

[3] D. Kusnezov, A. Bulgac, G. Do Dang, Quantum levy processes and fractional kinetics, Physical review letters 82 (6) (1999) 1136.

[4] M. Ichise, Y. Nagayanagi, T. Kojima, An analog simulation of non-integer order transfer functions for analysis of electrode processes, Journal of Electroanalytical Chemistry and Interfacial Electrochemistry 33 (2) (1971) 253–265.

[5] R. Metzler, J. Klafter, The random walk's guide to anomalous diffusion: a fractional dynamics approach, Physics reports 339 (1) (2000) 1–77.

[6] F. Mainardi, Fractional relaxation-oscillation and fractional diffusion-wave phenomena, Chaos, Solitons & Fractals 7 (9) (1996) 1461–1477.

[7] J. Gómez-Aguilar, J. Rosales-García, J. Bernal-Alvarado, T. Córdova-Fraga, R. Guzmán-Cabrera, Fractional mechanical oscillators, Revista mexicana de física 58 (4) (2012) 348–352.

[8] W. Ahmad, R. El-Khazali, A. Elwakil, Fractional-order Wien-bridge oscillator, Electronics Letters 37 (18) (2001) 1110–1112.

[9] A. Allagui, A. S. Elwakil, B. J. Maundy, T. J. Freeborn, Spectral Capacitance of Series and Parallel Combinations of Supercapacitors, ChemElectroChem 3 (9) (2016) 1429–1436.

[10] K. Biswas, S. Sen, P. K. Dutta, Realization of a constant phase element and its performance study in a differentiator circuit, IEEE Transactions on Circuits and Systems Part II Express Briefs 53 (9) (2006) 802.

[11] A. Radwan, A. Soliman, A. Elwakil, Design equations for fractional-order sinusoidal oscillators: Four practical circuit examples, International Journal of Circuit Theory and Applications 36 (4) (2008) 473–492.

[12] A. G. Radwan, A. S. Elwakil, A. M. Soliman, Fractional-order sinusoidal oscillators: design procedure and practical examples, IEEE Transactions on Circuits and Systems I: Regular Papers 55 (7) (2008) 2051–2063.

[13] L. Chen, W. Pan, R. Wu, K. Wang, Y. He, Generation and circuit implementation of fractional-order multi-scroll attractors, Chaos, Solitons & Fractals 85 (2016) 22–31.

[14] B. Maundy, A. Elwakil, S. Gift, On a multivibrator that employs a fractional capacitor, Analog Integrated Circuits and Signal Processing 62 (1) (2010) 99–103.

[15] A. Elwakil, A. Allagui, B. Maundy, C. Psychalinos, A low frequency oscillator using a super-capacitor, AEU-International Journal of Electronics and Communications 70 (7) (2016) 970–973.

[16] T. J. Freeborn, B. Maundy, A. S. Elwakil, Measurement of supercapacitor fractional-order model parameters from voltage-excited step response, IEEE Journal on Emerging and Selected Topics in Circuits and Systems 3 (3) (2013) 367–376.

[17] A. M. Elshurafa, M. N. Almadhoun, K. Salama, H. Alshareef, Microscale electrostatic fractional capacitors using reduced graphene oxide percolated polymer composites, Applied Physics Letters 102 (23) (2013) 232901.

[18] D. Mondal, K. Biswas, Packaging of single-component fractional order element, IEEE Transactions on Device and Materials Reliability 13 (1) (2013) 73–80.

[19] A. Adhikary, P. Sen, S. Sen, K. Biswas, Design and Performance Study of Dynamic Fractors in Any of the Four Quadrants, Circuits, Systems, and Signal Processing 35 (6) (2016) 1909–1932.

[20] M. N. Almadhoun, A. Elshurafa, K. Salama, H. Alshareef, Fractional order capacitor, uS Patent 9,305,706, 2016.

[21] S. G. Samko, A. A. Kilbas, O. L. Marichev, Fractional Integrals and Derivatives: Theory and Applications, CRC Press, 1993.

[22] K. B. Oldham The Fractional Calculus: Theory and Applications of Differentiation and Integration to Arbitrary Order, Dover Publications, 2006.